

Calibration of Nonlinear Response History Analysis Results With Observed Structural Damage in an Apartment Building in Chile



15 WCEE
LISBOA 2012

S.G. Bolaños-Castro

University College London (UCL), London WC1E 6BT, UK

D.N. Grant

Advanced Technology + Research Group, Arup, London W1T 4BQ, UK

SUMMARY:

After the Mw 8.8, 27 February 2010 Maule Earthquake in Chile, damage to an apartment building in Talca was extensively documented. In this study, observed damage to coupling beams in this building is classified according to a bespoke 5-level damage scale, based on photographs of all the beams and knowledge of their locations in the structure. Nonlinear response history analysis is carried out on a model of the building and results are processed in terms of several empirical damage scales from the literature. These results are compared with the observed damage classification, and it is shown that there is significant correlation between the observations and analysis model, with a Spearman rank coefficients of around 0.6. In this case, the damage scale due to Krawinkler and Zohrei gives the best correlation with observed damage. Although these correlations are specific to this application, they support the use of response history analysis and lend evidence to the use of empirical damage scales for seismic structural assessment of buildings.

Key words: damage scales, earthquake damage, nonlinear response history analysis, Maule earthquake

1. INTRODUCTION

Earthquakes are often described as experiments based on full scale shaking, albeit with less control over the input demand and structural properties. It is often difficult to collect robust data for subsequent study, particularly since data collection can interfere with higher priority activities, such as search and rescue and clean up. Earthquake reconnaissance efforts typically seek an overview of damage in an area to draw lessons for the design of structures in the future, and do not often have the time to document damage in a single building in the level of detail required for subsequent analysis.

As part of the Earthquake Engineering Field Investigation Team (EEFIT, 2010) fieldwork following the Mw 8.8, 27th of February of 2010 Maule Earthquake in Chile, a large body of data was obtained for an apartment building in Talca, the capital city of the Maule Region. Data available comprised structural drawings, material specifications and photos of damage to the building caused by the earthquake – mostly in coupling beams above apartment doorways. These data had been collected by the building administrator immediately following the earthquake, and were provided to the EEFIT investigators. Photos of coupling beam damage had been labelled with their position in the structure, and photos had been taken of almost every beam in the building.

This relative wealth of data allowed a relatively detailed analysis effort to be carried out on this building. In this study, observed damage to coupling beams was classified according to a bespoke 5-level damage scale, based on photographs of all the beams and knowledge of their location in the structure. Nonlinear response history analysis was carried out on a model of the building, and damage classifications were compared with the results of the analysis. The methodology and results of the study are summarised in this paper. More detail about the first stage of the study is available in Bolaños-Castro (2011).

2. CASE OF STUDY

2.1. Earthquake

In the morning of the 27th of February, 2010 an earthquake with moment magnitude 8.8 shook the Maule Region in Chile, South America. The earthquake had its epicentre 8 km off the Chilean coast, at a hypocentral depth of 35 km. The thrust-faulting focal mechanism is present along the entire 5000 km length of the western coastline of South America, known as the Peru-Chile trench and in this case the event was centred around 65 miles west-southwest of Talca, and 200 miles southwest of Santiago, and had a rupture zone of approximately 500-600 km with a displacement of almost 10 meters (Elnashai, 2010). The earthquake left nearly half the country declared as catastrophe zones and curfews were imposed in some areas due to looting and public disorder.

One month after the Maule earthquake, EEFIT sent a team to those areas affected by the earthquake regions of Chile. The aim of the expedition was to survey the region known as the Central Valley between the north of Santiago and south to the Rio Biobío. The report generated by the team of the mission includes a description of the factual findings from the earthquake in each of the main cities assessed as well as general conclusions regarding the subjects evaluated (EEFIT, 2010). The field trip took place from the 25th of March to the 3rd of April, 2010.

2.2. Study Building

During the EEFIT mission to Chile, one of the buildings surveyed was an apartment building in Talca, a few blocks from the city centre. The building is eighteen storeys high with two levels of basement. A Google Earth image is shown in Fig. 1(a). It includes six different apartment sizes as can be seen in Fig. 1(b). The building is L-shaped in plan, and there is movement joint between the two wings of the building. The structural system of the building is predominantly based on reinforced concrete (RC) structural walls (shear walls). Walls are coupled with beams above doorways, but these beams are relatively lightly reinforced, suggesting that they may not have been designed as energy dissipative elements. The walls are reinforced with a minimal ratio of reinforcement (0.25%), typical of buildings of this type with a large cross sectional area of walls. A detail of the wall and beams reinforcement can be seen in Fig. 2.

Although the building performance during the earthquake was generally in accordance with expectations for code-designed buildings in major earthquakes, there was heavy damage to coupling beams above the doors openings. As of the end of March, 2010, only 40 out of 250 units had been reoccupied, due to residents' concerns about the earthquake damage, and the perceived risk of aftershocks (EEFIT, 2010). A thorough systematic photographic record of the damage to the beams had been assembled by the building's administrator immediately following the earthquake. This data set, as well as access to the building's principal drawings, was the basis of the present study.



Figure 1. Study building. (a) Google Earth image; (b) plan and apartment layout of building.

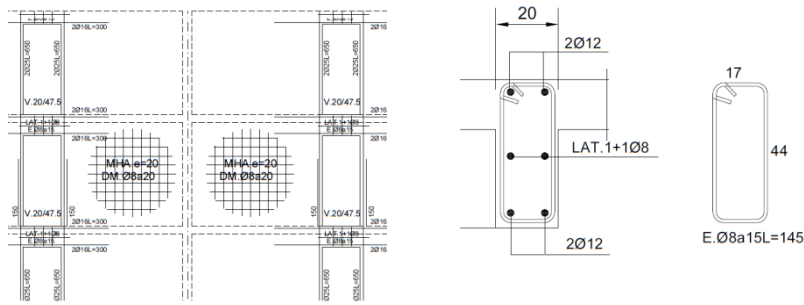


Figure 2. Distribution of reinforcement in walls and beams.

3. STRUCTURAL ANALYSIS MODEL

3.1. Ruaumoko Model Overview

A 2D structural model was developed using *Ruaumoko*, a general purpose non-linear dynamic analysis program (Carr, 2007). An inelastic response history analysis was carried out, using the Newmark constant average acceleration algorithm, with a lumped mass matrix, tangent stiffness Rayleigh damping of 5% of critical and including P-Delta effects. The model was set up for the gridline corresponding to the horizontal inner wall considered to be the critical one according to its structural distribution as it encompasses the entrance opening on the ground floor. Three-dimensional torsion effects were ignored. Figure 3 shows the model layout and the process of the analysis with the yielding of the elements marked with blue and red at a point of the ground peak acceleration.

3.2. Modelling of Elements

Walls were modelled with one-dimensional beam elements located at the centroid of each wall. Rigid offsets were used to model offsets from centrelines to the connection with coupling beams, as shown in Fig. 3. Member hysteresis and stiffness degradation was taken into account with the Modified Takeda hysteresis model, with γ and β parameters taken as 0.5 and 0, respectively, for the walls. The one-dimensional beams in the model were also defined with the Modified Takeda hysteresis rule, using γ as 0.3 and β as 0.6. Strength degradation for both beams and walls was taken as zero.

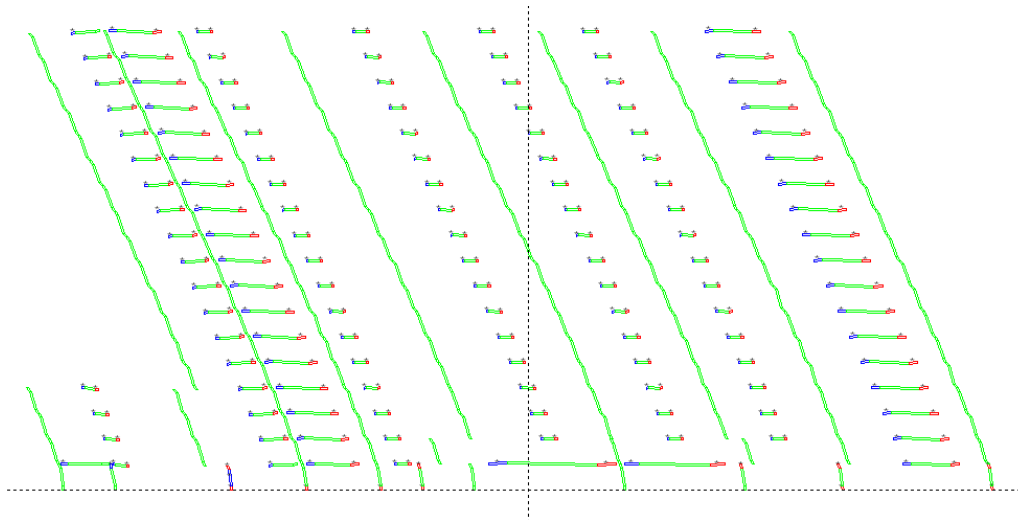


Figure 3. Screenshot from *Ruaumoko* showing arrangement of walls and coupling beams (both modelled with 1D beam elements). Red and blue colours represent yielding of plastic hinges at this point in analysis.

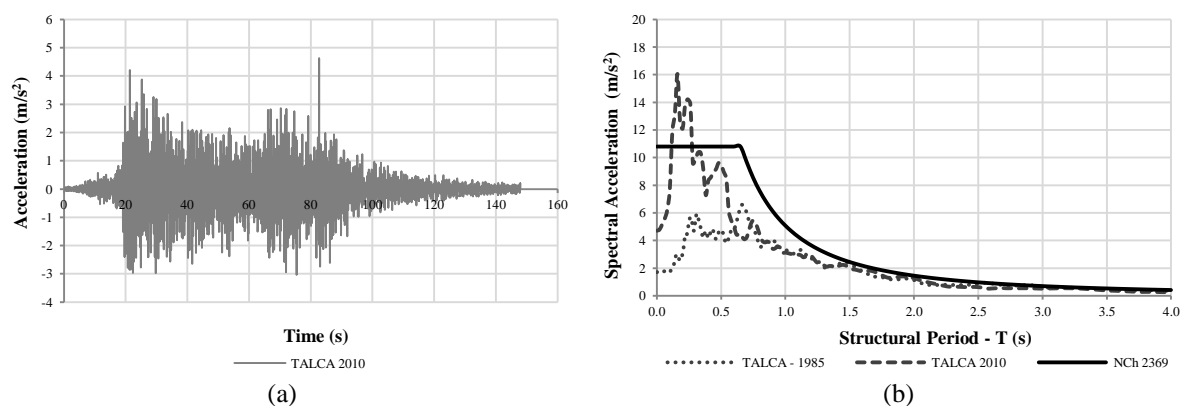


Figure 4. (a) Ground acceleration history recorded by the Talca Seismological Station. (b) Response spectra from Chilean code and at Talca station from Maule, 2010 and Valparaíso, 1985 earthquakes.

3.3. Ground Motion Input

The nearest ground motion recording station to the study building was the Talca station, located around 90 km (Cosmos, 2007) from the building. Clearly, the differing effects of site conditions and wave passage effects mean the record may not represent the exact amount of shaking that the structure experienced, but this is the most representative accelerogram available for the study. Fig. 4(a) shows the time series for the acceleration values of the Talca record and Fig. 4(b) shows the spectra of the event compared with the design spectra from Chilean code and with the Talca recording of the Valparaíso, 1985 earthquake for comparison. The spectra of the 2010 recording is comparable with both the 1985 recording and the Chilean code spectrum for periods greater than 1.5 seconds (as noted in Section 5, this is relevant to the study building with a period of 1.7 seconds).

4. PROCESSING OF RESULTS

4.1. Classification of Observed Damage

The damage suffered by the coupling beams was classified into five categories distributed from “No observable damage” to “Complete cover concrete spalling”. A bespoke damage scale was used for this purpose based on damage observable in the photographs. The damage scale was based on a classification of damage observed in this particular building, and is not calibrated against other scales in the literature. The defined damage states and a typical photo representing each one are described and shown in Fig. 5. As with other damage scales used in the literature, the assignment of numerical indices to different levels of damage does not mean that the scale is linear. These are simply a ranking of the minimum differences in degrees of damage that could be classified based on the photos alone.

Since the focus of the damage was located in the coupling beams, those photographs were the most pertinent and comprise a group of 335 photographs for the whole building, and 103 for the beams on the gridline considered in the analysis model for this study.



Figure 5. Damage states defined. 1. No observable damage. 2. At least one concrete crack. 3. Some cover concrete spalling. 4. Major cover concrete spalling. 5. Complete cover concrete spalling.

4.2. Classification of Damage from the Analysis Model

Building damage indices provide a quantitative measure of damage based on local response quantities in structural components, such as measures of plastic rotation and ductility, and cyclic energy dissipation. A number of indices were calculated for beams and structural walls in this study, and a brief description of each of them is given below.

4.2.1. Peak Ductility Ratio (D)

Peak ductility, μ , is one of the most commonly used measures of deformation, both in members and overall structures. Ductility is defined as:

$$\mu = \frac{D_m}{D_y} \quad (4.1)$$

where D_m is the maximum value of some displacement based parameter, and D_y is the yield value. In this study, values of curvature ductility calculated by *Ruaumoko* were used as a simple damage index to compare with observed damage.

4.2.2. Park & Ang (PA)

The Park & Ang (1985) damage index, commonly used for seismic assessment, is based on both the peak demand in the analysis and the energy absorbed by the members. Its value is determined from:

$$PA = \frac{\mu_m}{\mu_u} + \frac{\beta E_h}{F_y \mu_u \delta_y} \quad (4.2)$$

where μ_m and μ_u are the maximum and ultimate ductilities, β is a parameter defining relative importance of peak ductility and cyclic energy dissipation, E_h is total hysteretic energy dissipation, and F_y and δ_y are the yield force and yield curvature. In RC structures, the β parameter depends on the value of shear and axial forces in the section and on the total amount of longitudinal and confining reinforcement, and generally varies between -0.3 and $+1.2$. For this study, the value of β was taken as 0.1 (Ghosh, 2011).

4.2.3. Plastic Rotation (PR)

Plastic rotation is another simple, commonly used measure of damage. Current guidelines for performance-based seismic design, such as ASCE/SEI 41-06 use plastic rotation limits to assess different performance levels, such as “immediate occupancy”, “life safety” and “collapse prevention. These limits are modified based on the shear demand in the member, axial load, and presence of ductile detailing. Here, the plastic rotation was calculated by taking the *Ruaumoko* plastic curvature output and multiplying by an assumed equivalent plastic hinge length. Then this was normalised with respect to the ASCE/SEI 41-06 limit for “collapse prevention”, taking into account shear force output from *Ruaumoko*.

4.2.4. Bracci *et al.* (B)

Bracci *et al.* (1989) proposed a local damage index that attempts to account for the effects of cyclic loading or cumulative damage from consideration of strength degradation characteristics of the structure. The damage index is calculated as the difference between the areas under the monotonic load response curve and the cyclic load response envelope. *Ruaumoko* estimates the index from:

$$B \approx \frac{E_m}{E_u} \quad (4.3)$$

where E_m and E_u are the work done at maximum and ultimate ductility, respectively.

4.2.5. Roufaiel & Meyer (RM)

Roufaiel and Meyer (1987) suggested that the ratio of initial stiffness, the flexural damage ratio, to the reduced secant stiffness at the maximum displacement can be used as a measure of damage. Damage indices based on extreme inelastic deformations seem to be strongly correlated so that their predictions are usually similar (Ghobarah, 1999). The equation used by *Ruaumoko* to obtain this damage index is:

$$RM = \frac{\frac{\mu_m}{F_m} \frac{\mu_y}{F_y}}{\frac{\mu_u}{F_u} \frac{\mu_y}{F_y}} \quad (4.4)$$

where μ_m , μ_y , F_m , F_y and F_u are the maximum and yield ductilities, the maximum, yield and ultimate actions, respectively.

4.2.6. Cosenza & Manfredi (CM)

Cosenza & Manfredi (1993) proposed a damage factor related to the number of plastic cycles, n , and therefore, to the energy content of the earthquake (Estekanchi, 2007). Eq. (4.5) represents the calculation carried out by the software, where the parameters are defined as before.

$$CM = \frac{\mu_m^{-1}}{\mu_u^{-1}} \quad (4.5)$$

4.2.7. Banon and Veneziano (BV)

Early deformation-based indices tried to account for cumulative damage by extending the concept of ductility for repeated loadings. Banon and Veneziano (1982) proposed the normalised cumulative deformation as a damage index. This index is defined as the ratio of the sum over all half-cycles of all the maximum plastic deformations to the deformation at yield as follows (Estekanchi, 2007):

$$BV = \frac{\sqrt{\left(\frac{\mu_m}{\mu_y} - 1\right)^2 + \left(1.1 \left(\frac{2E_p}{F_y \mu_y}\right)^{0.38}\right)^2}}{\text{the numerator for monotonic loading}} \quad (4.6)$$

4.2.8. Krawinkler and Zohrei (KZ)

It is convenient to use cumulative damage models to predict the probability of failure in cyclically loaded materials or structural elements. Krawinkler and Zohrei (1983) introduced a damage index using three kinds of deterioration in an element to define its damage, i.e. strength, stiffness and energy dissipation capacity (Estekanchi, 2007). This is calculated in *Ruaumoko* as follows:

$$KZ = \frac{\sum(\mu_j - 1)^{1.5}}{(\mu_u - 1)^{1.5}} \quad (4.7)$$

where μ_j is the ductility in cycle j , and μ_u is the ultimate ductility.

4.3. Statistical Analysis

Spearman's rank-order correlation coefficient measures the strength of association between two ranked variables (Spearman, 1907). It does not require the data to be linearly related or continuous and therefore it is adequate for these data where we have damage indices that do not have a numerical meaning. Spearman's correlation coefficient was calculated to measure correlation between each of the calculated and observed damage indices using the computer program IBM SPSS Statistics 20 (USA, 2011) and the values were considered as significant if $p < 0.05$.

5. RESULTS AND DISCUSSION

5.1. Overall Results

The structural analysis model gave a fundamental period of the structure of 1.72 seconds – a reasonable value for a building of this height and structural system. From the *Ruaumoko* output, the main storey forces were processed. The distributions of moment, shear and interstorey drift are shown in Fig. 6. Figs. 6(a) and (b) show a reasonably uniform distribution of moment and shear up the height of the structure, while Fig. 6(c) shows a relatively low interstorey drift in the bottom storey, but much higher drift for the second level in above, in excess of the 1.5% limit of the Chilean code NCh2369 (2003), were present. Unfortunately 1st level coupling beams were not documented, so we cannot tell if the damage experienced by these beams reflects the lower drift at this level. We also did not have photos of walls – either at base level (where drift is smaller) or at the base of the 2nd level, where we may expect damage to be concentrated according to the sharp change in drift at this level.

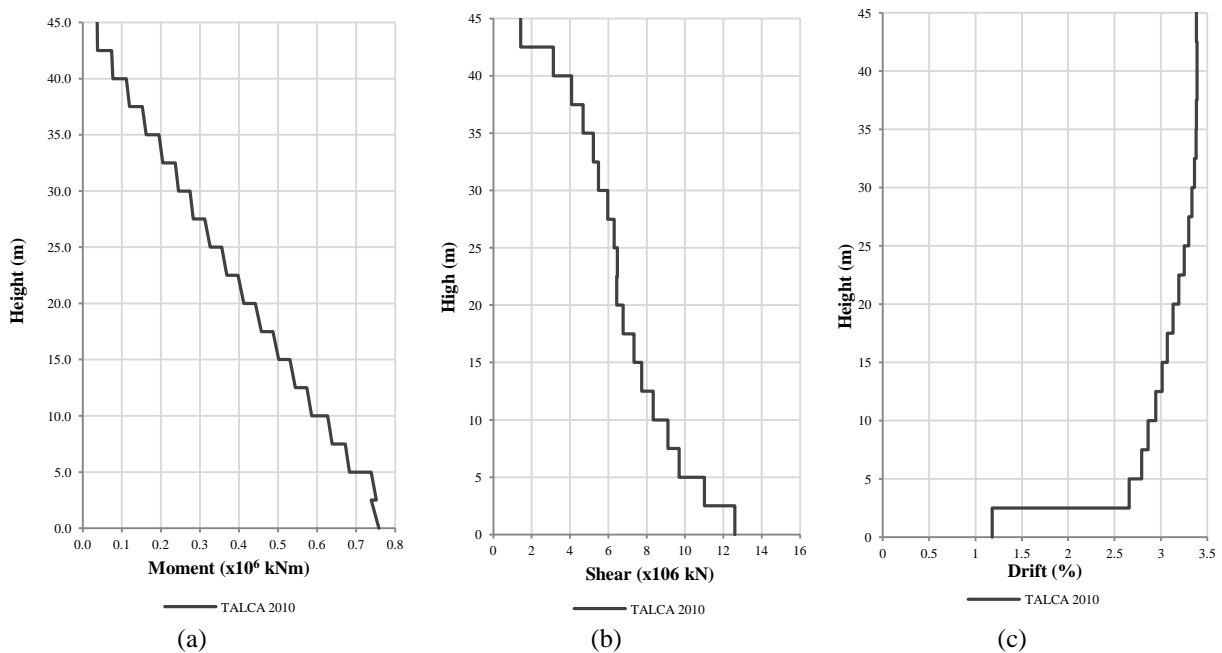


Figure 6. (a) Moment force felt by the structure. (b) Shear force felt by the structure. (c) Drift ratio suffered by the structure.

5.2. Beams

As mentioned, the beams were first classified in five categories according to the observable damage from the photographs taken of each apartment doorway. The observed damage distribution after the event is shown in Fig. 7(a) and the central area of the building can be identified as the most damaged one, since all the beams are classified as Level 5. The damage distribution does not change significantly up the height of the building, which is consistent with the drift distribution in Fig. 6(c). The calculated damage distribution for the Krawinkler and Zohrei damage index is shown in Fig. 7(b), and shows that the overall distribution of damage has been calculated reasonably well by the analysis model and damage index calculation, although there are some discrepancies.

One source of potential error to point out from the study is the active subjectivity of the observed damage classification. Furthermore, there are several variables that could affect the appreciation of the damage on the beams as the camera quality, lighting conditions, distance, etc. Still, these are conditions assumed to be relatively constant across all photos. The idea here was to provide a relative measure which could be useful for ranking the damage observable in the photos. At the same time, the ground motion experienced by the structure could have been affected by site effects.

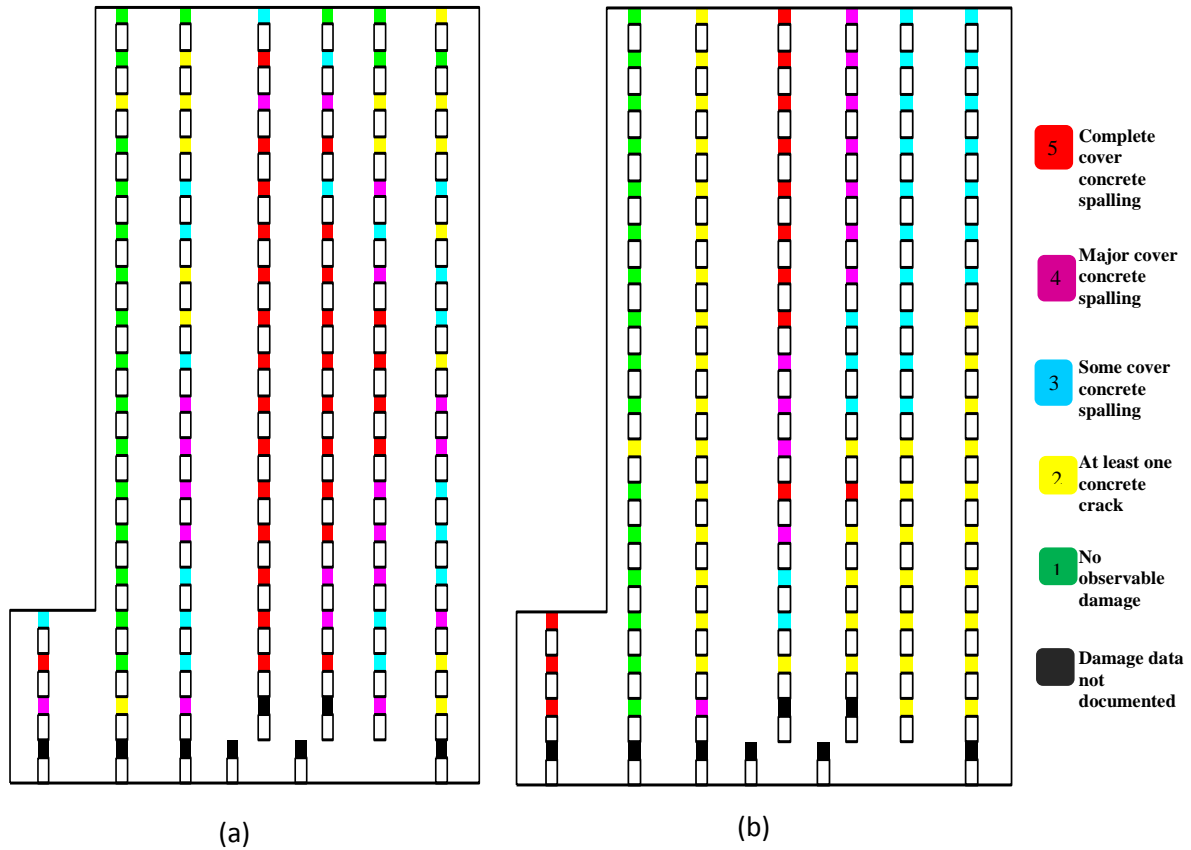


Figure 7. (a) Observed damage classification from photographs. (b) KZ empirical damage distribution.

In addition, the eight empirical damage indices described above were calculated for each beam. The Spearman’s correlation coefficient was calculated between each damage index and the observed damage classification of the beams. The results for each of the beam hinge empirical damage and for the average values of both hinges correlation coefficients are shown in Table 5.1. All of the correlations were statistically significant ($p = 0.001$). The Krawinkler and Zohrei damage index has the best correlation coefficient between observed and calculated damage. Each end of the beam is evaluated separately, and the average value is also reported. Generally, the values for each end are close. The damage indices sensitive to the member ultimate curvature ductility, such as Park & Ang, Banon & Veneziano, Roufaiel & Meyer and Cosenza & Menefredi, as expected, presented very similar correlations and consequently, comparable to the deformation index as well.

Table 5.1. Data for Spearman’s correlation coefficient between each damage index and the observed damage for each hinge of the beams, their average value and average when Level 18 data is removed.

	D	PA	PR	B	RM	CM	BV	KZ
End 1	0.552	0.528	0.289	0.238	0.552	0.552	0.504	0.607
End 2	0.555	0.528	0.318	0.338	0.556	0.556	0.508	0.590
Average	0.551	0.528	0.301	0.205	0.552	0.552	0.509	0.606
Average without L18	0.635	0.623	0.354	0.262	0.637	0.636	0.613	0.683

The observed damage versus calculated damage index is shown in Fig. 8. Values from Level 18 (highlighted in red) are outliers on this plot, where the observed damage was significantly lower than calculated in the analysis model. A possible explanation for this is that there is additional structure at the top floor supporting boilers and equipment, and this was not modelled in the structural analysis model, which just focused on the lateral load resisting system on a single gridline. The Spearman correlation coefficients with Level 18 data removed are also shown in Table 5.1, and it is seen that this improves the correlation.

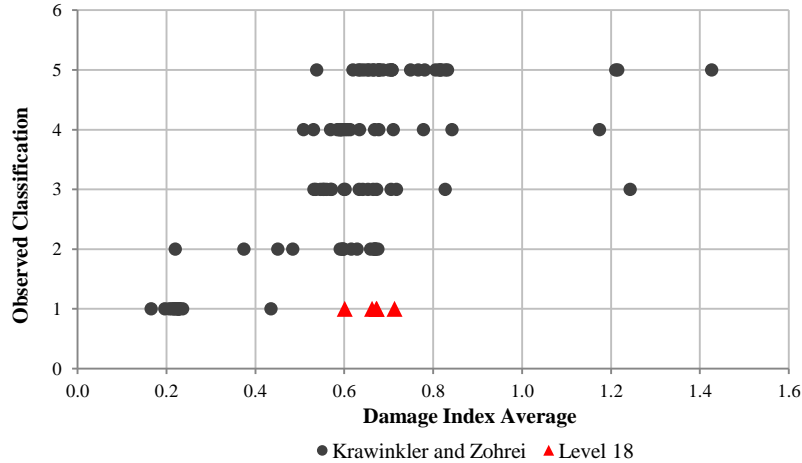


Figure 8. Correlation diagram between the observed damage and the Krawinkler and Zohrei damage index.

5.3. Walls

In the analysis model, the ground floor walls, especially the second from the right, yielded at the base, with plastic rotations of up to 0.1 radians. The corresponding peak shear stress in the walls was up to 3 MPa, which is around 70% of the maximum value allowed by ACI 318 for structural walls with this concrete grade. The walls actual damage was not photographically recorded or officially reported. This could be because the damage in the walls was not as significant as the more extreme levels of coupling beams damage stated, or alternatively that damage was in a position on the wall that was not observable or noticed. According to the rough correlation determined between the calculated Krawinkler and Zohrei index, and the observed beam damage (Fig. 8), some of the middle walls would have been expected to show damage equivalent to what was classified as Level 3 in the beams.

6. CONCLUSIONS

This study pursued the comparative analysis of two strategies for structural damage assessment: the damage observed *in situ* after the Maule earthquake, Chile, 2010, and the expected damage calculated from empirical equations using the output data from a non-linear response history analysis. The paper compared the distribution of damage observed in a building in Talca, classified according to a 5-level damage scale, with damage indices available from the literature. A reasonable correlation of the damage distributions was obtained, lending support to the use of empirical damage scales for structural assessment, considering the relative simplicity of the nonlinear model adopted.

The study could be improved by carrying out a full 3D model of the structure, including torsional effects, and potentially pounding across the movement joint interface. On the other hand, the main limitation to the sophistication of the modelling that can be adopted is that the ground motion recording was measured some distance from the structure, and no site data is available to determine if the level of shaking applied in this model is representative of what was experienced during the 2010 earthquake.

ACKNOWLEDGEMENTS

We would like to thank Mr. Cristián Ilufi, manager of the building at the time of the Maule earthquake, Chile, 2010, for providing the data to the EEFIT team during their reconnaissance mission, and further supporting this research work while it was being carried out. The second author would also like to thank the other members of the EEFIT mission team, particularly Tristan Lloyd, who visited the building with him.

REFERENCES

- Banon, H., Biggs, J.M., and Irvine, H.M. (1981). Seismic damage in reinforced concrete frames. *Journal of Structural Engineering. ASCE*, **107:9**,1713–1729.
- Barroso, L. (1999). *Performance evaluation of vibration controlled steel structures under seismic loading*. Dissertation Project. Doctor of Philosophy. Civil and Environmental Engineering. Stanford University, USA.
- Bolaños-Castro, S. (2011). *Calibration of nonlinear response history analysis results with observed structural damage in 2010 Maule (Chile) Earthquake*. Dissertation Project. MSc. Earthquake Engineering with Disaster Management. University College London. UK.
- Bracci, J.M., Reinhorn, A.M., Mander, J.B., and Kunnath, S.K. (1989). *Deterministic model for seismic damage evaluation of RC structures*. Report No. NCEER:89:0033, National Center for Earthquake Engineering Research, State University of New York, Buffalo, USA.
- Carr, A. (2007). *User Manual for the 2-Dimensional Version, Ruaumoko 2D. Inelastic Dynamic Analysis*. University of Canterbury.
- Cosenza, E., Manfredi, G., and Ramasco, R. (1993). The use of damage functions in earthquake engineering: A comparison between different methods. *Earthquake Engineering and Structural Dynamics*, **22**, 855–868.
- Cosmos Virtual Data Center (2007). *Consortium of Organizations for Strong-Motion Observation Systems*. The Regents of the University of California.
- Dong, P., Moss, P. (2003) Seismic structural damage assessment of reinforced concrete ductile frame structures. *Pacific Conference on Earthquake Engineering*, New Zealand. **Paper number 075**.
- Earthquake Engineering Field Investigation Team. EEFIT. (2010). *The Mw8.8 Maule Chile Earthquake of 27th February 2010*. The Institution of Structural Engineers. UK.
- Elnashai, A., Gencturk, B., et al. (2010). *The Maule (Chile) Earthquake of February 27, 2010: Consequence Assessment and Case Studies*. Mid-America Earthquake Center MAE Center. Report No.10-04
- Estekanchi, H. and Arjomandi, K. (2007). Comparison of damage indexes in nonlinear time history analysis of steel moment frames. *Asian Journal of Civil Engineering (Building and Housing)*. **8:6**, 629–646.
- Ghobarah, A., Abou-Elfath, H. and Biddah, A. (1999). Response-Based damage assessment of structures. *Earthquake Engineering and Structural Dynamics*. **28**, 79–104.
- Ghosh, S., Datta, D., et al. (2011). Estimation of the Park-Ang damage index for planar multi-storey frames using equivalent single-degree systems. *Engineering Structures*. **33**, 2509–2524.
- Krawinkler, H. and Zohrei, M. (1983). Cumulative damage in steel structures subjected to earthquake ground motions. *Computers and Structures*, **16**, 531–541.
- Park, Y., Ang, F. (1985). Mechanistic Seismic Damage Model for Reinforced Concrete. *Journal of Structural Engineering ASCE*, **111:4**, 740–757
- Roufaiel, M.S.L., and Meyer, C. (1987). Analytical modeling of hysteretic behavior of RC frames. *Journal of Structural Engineering*. **113:3**, 429–444.
- Spearman, C. (1907). Demonstration of formulæ for true measurement of correlation. *The American Journal of Psychology*. **18:2**, 161–169.